Passive Control of Laminar Bubble Separation for S809 Wind Turbine Airfoil via Slot

R. MDOUKI[a]

a. Université Cheik Larbi Tébessi, Laboratoire Energétique et Turbomachines
mdouki_ramzi@yahoo.fr

Résumé :

Ce papier explore à travers une simulation numérique le phénomène du bulbe de séparation laminaire en utilisant le mailleur Pointwise et le solveur AnsysFluent. Sous un régime stationnaire, le solveur RANS incompressible est choisi avec le modèle de turbulence d'intermittence γ-Re SST *basé sur des corrélations empiriques dans le but de prédire l'aspect de la couche limite transitionnelle. Le profil aérodynamique utilisé dans les calculs représente le S809 de la pale d'éolienne à axe horizontal. Les tests numériques sont effectués à un nombre de Reynolds de 0.75 10^6 et une intensité turbulente de 0.3%. En fait, la présence du bulbe de séparation laminaire BSL exige l'intervention des techniques de contrôle pour diminuer voire éliminer cette zone de séparation-réattachement et par conséquent améliorer les performances aérodynamiques de la pale. Une technique originale de contrôle passif avec double fentes est proposée pour tester son potentiel devant le BSL développé sur les deux faces du profil sous un faible angle d'attaque. Les résultats sans contrôle ont été validés par des données expérimentales en donnant une bonne concordance. Concernant, le contrôle, la pale avec fentes possède un potentiel pour manipuler la BSL, néanmoins, elle ne peut pas conduire à des améliorations significatives des performances aérodynamiques à cause de la taille de la BSL.*

Abstract : (16 gras)

This paper explores through a numerical simulation the laminar bubble separation phenomena using Ansys Fluent and pointwise codes. Under steady regime, pressure based RANS solver was selected with correlation-based intermittency turbulent model in order to predict the boundary layer transition aspect. The aerodynamic profile used in calculation represented an S809 horizontal axis wind turbine airfoil. The numerical tests were carried out for Reynolds number of 0.75 10^5 and Turbulence intensity of 0.3%. In fact, the presence of the laminar bubble separation required the use of control device to mitigate or delete this separation-reattachment zone and therefore enhancing the aerodynamic performance blade. Original passive control technique was proposed to testify its potential in front of the LSB developed over the two airfoil sides under small angle of attack. The control is fullfiled via tandem Slot within airfoil. The results without control were validated with experimental data and showed a good agreement. Concerning the control, the slotted airfoil has a potential to manipulate the LSB, however, it could not lead to a significant improvement of the aerodynamic performances because of the small size of the LSB.

Mots clefs : Slotted airfoil, LBS, S809, HAWT

1 Introduction

There are many applications such as wind turbines, Unmanned air vehicles and turbomachinery blades are characterized by a development of laminar separation bubble under low Reynolds number conditions. In fact, in the case of low Reynolds airfoil, laminar flow near leading edge is prone to separation under weak pressure gradients. Beyond the point of minimum pressure, laminar boundary layer is exposed to advrese pressure gradients and separation takes place. Due to the increase in level of velocity disturbances, the separated shear layer passes by transition phenomenon and unstable regime to generate turbulent shear layer that has the possibility to reatach and produce an enclosed zone known as separation bubble. This type of transition developped on the airfoil surface is named the separation-induced transition [1]. Usually, the extent and position of the separation bubble depends on airfoil geometry, global Reynolds number, turbulence intensity and angle of attack [1,2]. Over the Reynolds number range varying from 10^4 to 10^6, the two types of Laminar Separtion Bubbles LSBs either Short Laminar Separation Bubbles SLSBs or Long Laminar Separation Bubble LLSBs can be appeared and lead to deteriorate the aerodynamic performances of the airfoil. With the increasing of the angle of attack and/or the decreasing of the Reynolds number, the size of SLSBs decreases and its location moves towards the leading edge with the possibility to burst the SLSB and lead to airfoil stall accompanied with a LLSBs. Therefore, the application of suitable control technique to mitigate or delete the LSBs and avoid their noxious effect is necessary. The passive control technique via slots applied by the author on both compressor blades and wind turbine airfoils in works [3], [4] is proposed in the current study with a novel form and is aimed for the control of LBS developed on both suction and pressure sides of the wind turbine airfoil.

2 Investigation with Clean Airfoil

2.1 Geometry and Grid Generation

The S809 Horizontal Axis Wind Turbine airfoil is used in this study as an aerodynamic profile. It is qualified of laminar flow airfoil based on relative thickness of 21%. In this pre-processing step, Pointwise Package is selected to generate 2D structured mesh around the NREL S809 airfoil.

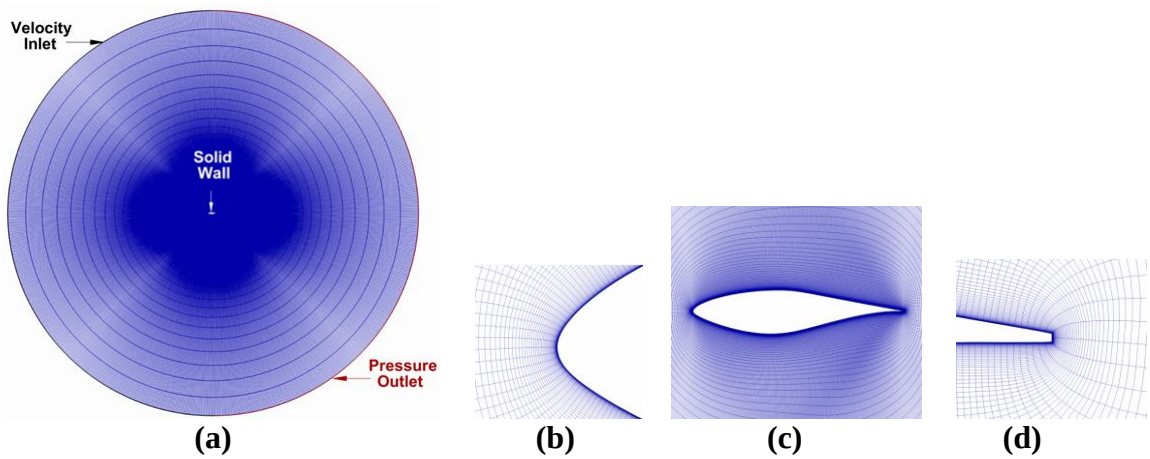

Fig. 1. (a) Overall grid and boundary conditions, (b) Enlarged view at leading edge, (c) mesh around S809 profile, (d) Thickened trailing edge

The flow field is discretized using hyperbolic extrusion with an O topology in order to provide lower skweness, minimize the number of cells, accelerate the convergence and increase the degree of control and accuracy. The airfoil is centered in the circular geometric domain while the boundaries are located 40 chord lengths far away from airfoil to avoid the effect of boundaries on the flow characteristics, fig.1.a. The flow is modeled by dividing it into 350.000 cells with 801 points imposed in the circonferential direction on each side of airfoil and 235 points in the radial direction. To capture the flow features in the severe gradient regions such as transition zone and viscous sub-layer, the model needs to adjust the thickness of neighboring elements to the airfoil surface with the value of 10^{-5}m in order to satisfy the condition $y^+ \leq 1$, fig.1.b, c and d.

2.2 Numerical Scheme and Boundary Conditions

In the processing step, the ANSYS-FLUENT solver is used as a CFD-tool for solving the governing equations. The flow model considered in the present investigation is based on two dimensional configuation, steady state, incompressible regime and RANS-based transition model. Therefore, the governing equations representing the transport of mass, momentum and turbulent quantities are discretized using the cell centered finite volume approach with second order upwind scheme applied in the space dimension. It is convenient to use with this model the two boundary conditions ; velocity inlet and pressure outlet. At the inlet, the velocity components, turbulence intensity and hydraulic diameter are specified. On the other hand, the velocity components and turbulence parameters are extrapolated from neighboring interior cells at the outlet. At solid walls such as pressure and suction surfaces ; the no slip and impermeability condition is imposed, fig.1.a. In the time dimension, assuming that LSBs are developped without vortex shedding, the simulations are performed starting from initial condition, which takes the values from inlet boundary, to reach steady state.

2.3 Turbulence Modelling with Transition

According the results obtained in the work of S.M.A. Aftab et al. [5], a set of tubulent models such as Spalart-Almaras, SST K-ω, γ-SST, k-k_L-ω, γ-Re SST were used to analyze the low Reynolds number flow on NACA4415 airfoil. The γ-Re SST model was chosen as preferable turbulent model to predict the transition behavior at both low and high AoA with accurate results and small convergence time. Therefore, the γ-Re SST model is adopted in our study. In fact, this model represent a combination of experimental correlations with local transport equations. The first two equations are the same as in the SST k-ω model. The transport equation for intermittency is used to trigger the transition process and manipulate the onset and extent of the transition. Menter et al [6] proposed the folowing expression :

$$\frac{\partial(\rho\gamma)}{\partial t}+\frac{\partial(\rho u_j\gamma)}{\partial x_j}=P_{\gamma 1}-E_{\gamma 1}+P_{\gamma 2}-E_{\gamma 2}+\frac{\partial}{\partial x_j}\left[\left(\mu+\frac{\mu_t}{\sigma_\gamma}\right)\frac{\partial\gamma}{\partial x_j}\right] \quad (1)$$

Concerning the transport equation for momentum thickness Reynolds number at the transition onset, it is expressed as :

$$\frac{\partial(\rho \mathrm{Re}_{\theta t})}{\partial t}+\frac{\partial(\rho u_j \mathrm{Re}_{\theta t})}{\partial x_j}=P_{\theta t}+\frac{\partial}{\partial x_j}\left[\sigma_{\theta t}(\mu+\mu_t)\frac{\partial \mathrm{Re}_{\theta t}}{\partial x_j}\right] \quad (2)$$

The interaction between transition model and SST k-ω is performed by modifying the production and destruction terms from the original SST model using the effective intermittency.

2.4 Validation of Clean Airfoil and Grid Independence Check

This study focuses on 2D numerical simulation of flow separation-induced transition and control over S809 airfoil at angles of attack corresponding to the case before the bursting of laminar bubble. The independence grid-solution is obtained after several attempting improvements for the configuration of 6.2^0 of angle of attack . Three factors are considered ; first, for all grids, thickness of neighboring cells *dy0* at airfoil surface is maintained to 10^{-5}m to ensure that $y^+ \leq 1$. Second, the number of points *naf* on each of the airfoil surfaces takes the five values between 101, and 501 with an ancrement of 100. Third, the effect of boundary location on the flow characteristics is taken into account ; three values representing the distance *dff* between the farfield and the airfoil are used 20, 30 and 40 chord lengths. Besides, both drag and lift coefficients are monitored as a check parameters of grid independence. The study results of grid-solution independence are shown in table 1. As can be observed in the table 1, that the variation in values of aerodynamic performances Cl and Cd is negligible between the generated grids and these values are almost the same as the experiment (Cl=0.79, Cd=0.013) for the majority of meshes. Except the first grid, the simulation could be performed with one of the grids such as G3.

Grid	*naf*	*dff*	*dy0*	*Cl*	*Cd*
G1	101	20c	10^{-5}	0.73	0.019
G2	201	20c	10^{-5}	0.78	0.014
G3	301	20c	10^{-5}	0.79	0.013
G4	401	20c	10^{-5}	0.79	0.013
G5	501	20c	10^{-5}	0.79	0.013
G6	301	30c	10^{-5}	0.80	0.012
G7	301	40c	10^{-5}	0.80	0.012

Table. 1. Grid-solution independence study

However, the pressure coefficient distribution reveals the oscillations in the zone of separation laminar bubble in the different grids and thus leads to a bad prediction of phenomenon. Therefore, the mesh that will be used in simulation, after tests, is characterized by *naf=801* and *dff=40c* and *dy0=10-5m*. To validate the numerical model ; a comparison between computational and experimental results is carried out for angle of attack 6.2^0. The experimental data comes from the Ramsey's report [7].

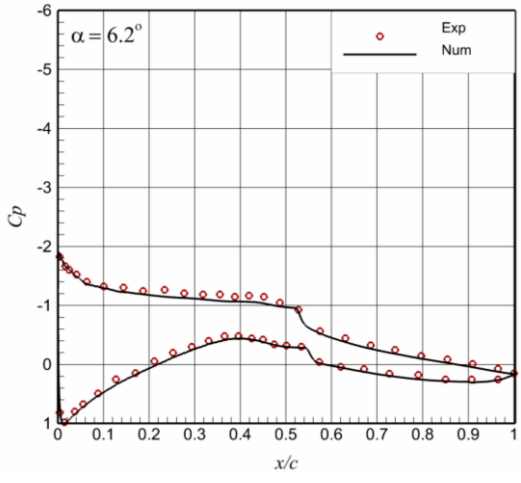

Fig. 2. Surface pressure coefficient distribution

The comparison is shown in fig.2 for the surface pressure distribution on a S809 airfoil without control and reported in terms of static pressure coefficient, Cp. The freestream conditions are set at Reynolds number Re=750000, based on blade chord c=0.457m. The shown result in Figure 1 give a good agreement with experimental data cited in [7].

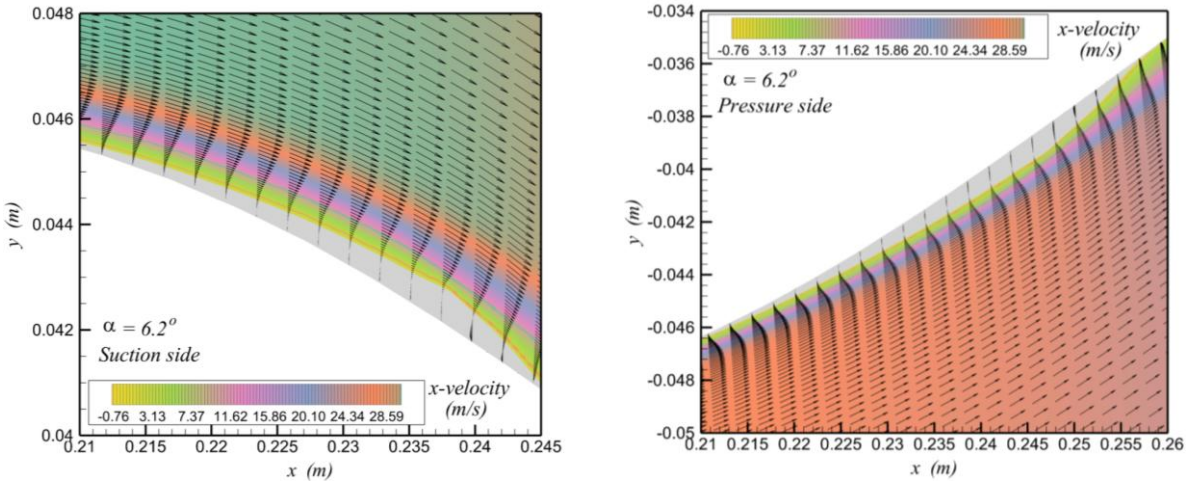

Fig. 3. Velocity vectors and countours for clean airfoil in LSB region over extrados (left) and intrados (right)

The flow field with velocity vectors in the region of LSB is plotted for extrados and intrados, fig. 3. It can be observed that the reverse flow with gray contour is between the laminar separation point at 47.8%c and 47.6%c for the upper and lower airfoil surfaces, respectively, and the reattachment point at 53.6%c and 55.9%c for the suction side and the pressure side, respectively, fig. 4. According to the length of two LSBs, they are classified as short bubbles. The separation of laminar boundary layer, transition onset and turbulent reattachment are identified using the x-wall shear stress distributions, as are illustrated in the thereafter figure.

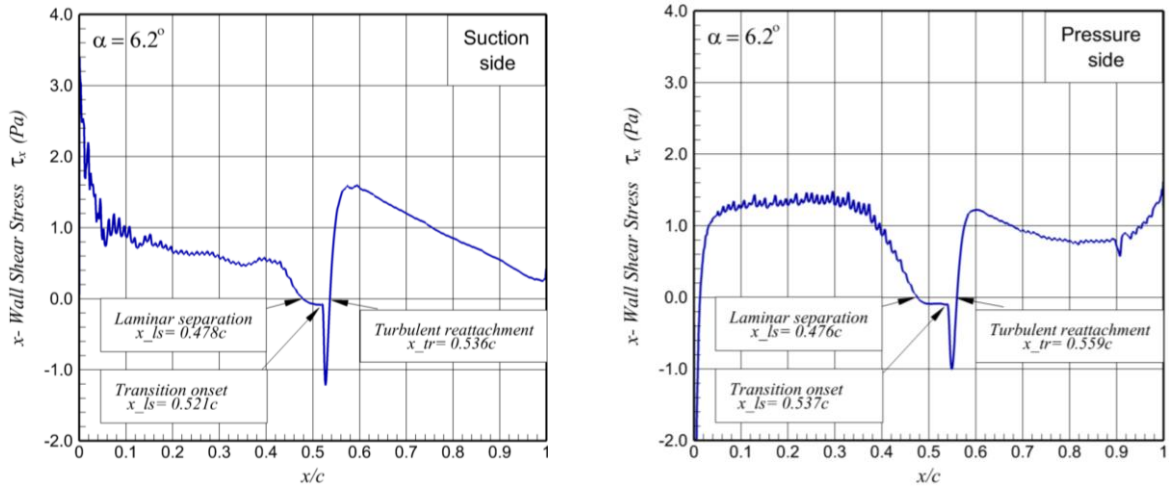

Fig. 4. X-Wall shear stress distribution over extrados (left), intrados (right)

The artificial production of turbulence in γ-Re SST model give high mixing and exchange of momentum that predicts an earlier reattachment of the detached shear layer. This feature is confirmed

in the figure 2 using the surface pressure distribution where it can be observed that the experimental curve is little more flattened comparing with the numerical one in the region of LSB.

3 Investigation with Slotted Airfoil

With the aim to control the LSB, NREL S809 airfoil is used as cross section caracterized by the chord length c=0.457m, maximum relative thickness of 21% and two slots implanted inside the airfoil such as schematized in the following figure.

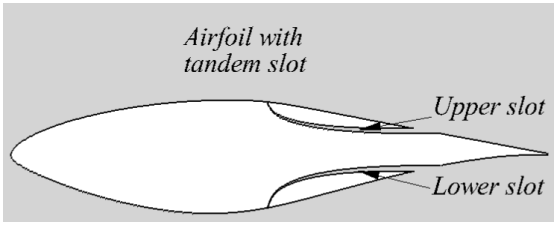

Fig. 5. S809 airfoil with tandem slot

Both entry and exit of slot in the two airfoil sides encompassed the locations 75%c - 80%c and 48%c - 48.125%c, respectively. The widths of the slot inlet and slot outlet are 5%c and 0.125%c.

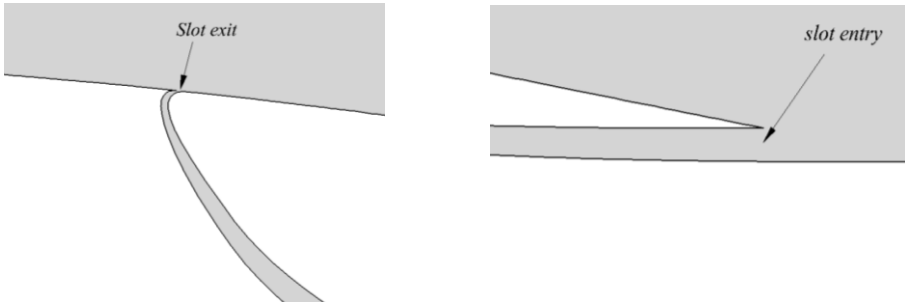

Fig. 6. Enlarged views of slot inlet and slot outlet

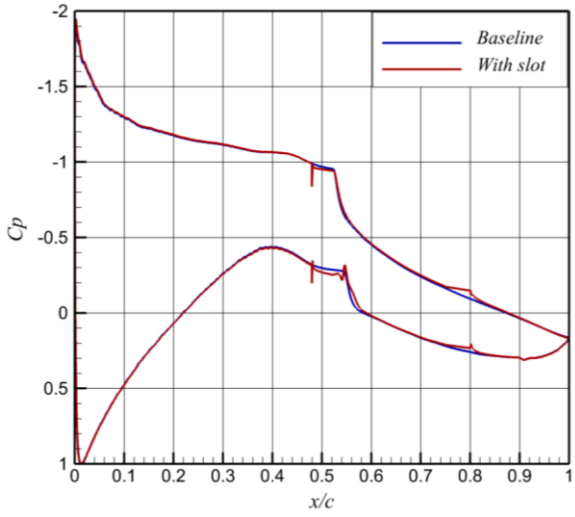

Fig. 7. Surface pressure coefficient distribution with and without control.

Figure 7 shows the distribution of pressure coefficient Cp over the airfoil. After this figure, the simulation indicates that the addition of tandem slot has only minor influence in the Cp distribution. Except near the slot inlet and outlet, the Cp of the baseline and controlled airfoil concides. Therefore, the effect of slot is negligeable to improve the pressure distribution and aerodynamic performance ; the lift and drag coefficients take approximately the same values : Cl_{clean}=0.778 - Cl_{slot}=0.785 and Cd_{clean}=0.0128 - Cd_{slot}=0.0122. According the figure 8, the x-wall shear stress distribution shows the positif effect of slot to delete the laminar separation zones on both extrados and intrados with the high mixing (positif pick of shear stress) which leads the flow in the boundary layer directly to the transition. Figure 9 illustrates the effect of slot with the high velocity jet represented in the vector field and contour. After this commentary, the only important remark is appears such as an ambiguity between the delete of laminar separation bubble and the not improving of the aerodynamic performance. In fact, the cause of this depends on the size of the LSB. Seemingly, the existence of the short bubble separation developed on the airfoil can not alter its performance.

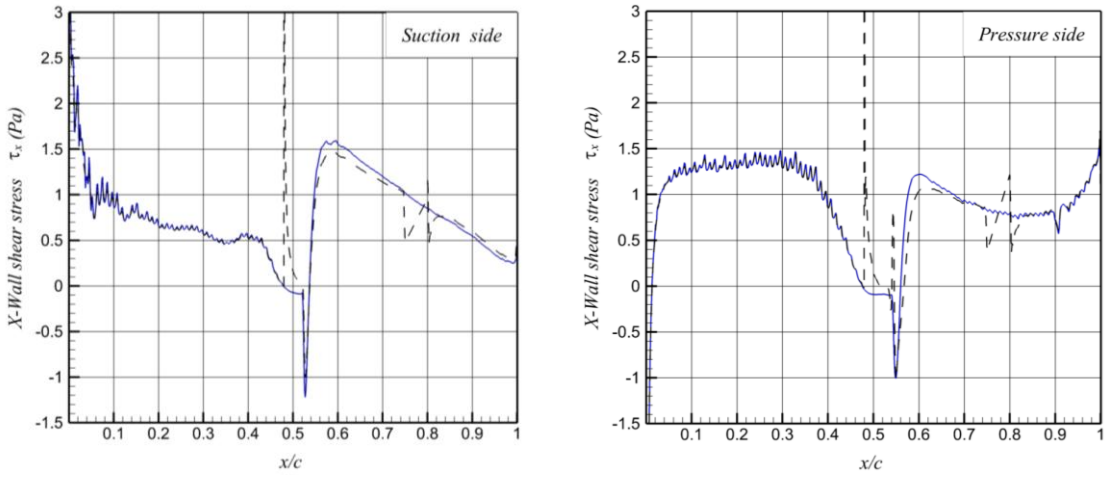

Fig. 8. Comparaison of X-Wall shear stress distribution over extrados (left), intrados (right) between baseline and slotted airfoil

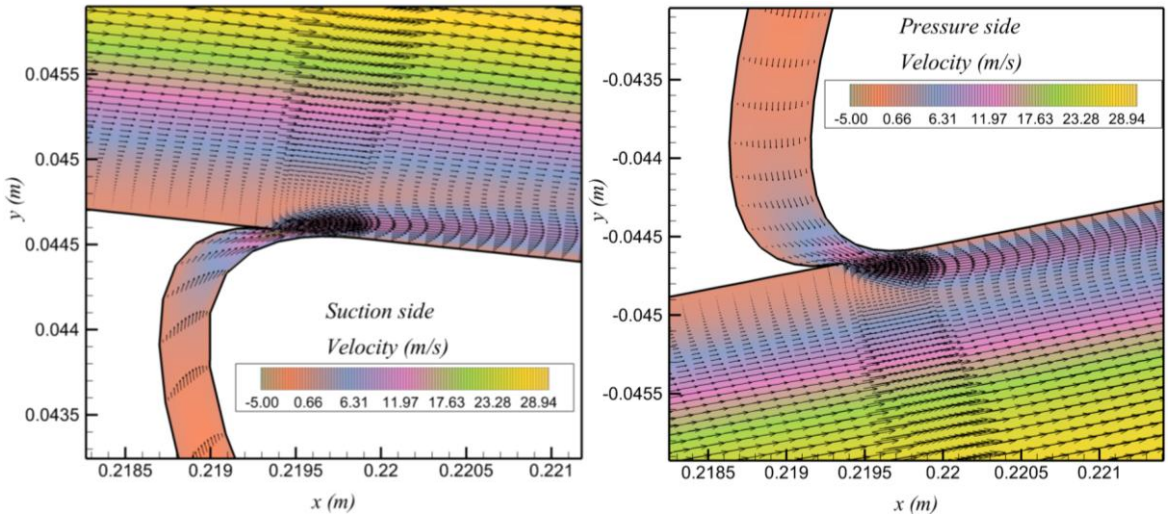

Fig. 9. Velocity vectors and countours for slotted airfoil in LSB region over extrados (left) and intrados (right)

4 Conclusion

Comparing the experimental and numerical results for the baseline configuration, correlation-based intermittency turbulent model seemed promising to predict the flow behaviour under low Reynolds number. For small angle of attack, simulation reveals the development of short laminar separation bubble on both pressure side and suction side. Tandem slot executed within airfoil was used to control the laminar bubble separation. Physically, this type of control attempts to manipulate passivelly the LSB, by linking the zone high pressurized near trailing edge with the region near upstream laminar separation point by two slots. Under the effect of pressure gradient between the slot inlet and slot outlet the flow exhausts tangentially and adds some momentum to the depleted fluid strata in order to minimize or delete the zones of boundary layer separation. Fortunately, the simulation showed that control via tandem slot is effective, in the chosen configuartion, to control the LSB. However, with the small size of LSB predicted numerically in this investigation, the slot could not lead to a significant inhancement in neither lift cofficient nor drag coefficient. Furthermore, the slotted airfoil yields to keep almost the level of mixing loss and the airfoil load as in the baseline case. The agree between the delete of laminar separation bubble and the not improving of the aerodynamic performance resides in the short size of the LBS. In fact, the present study gives an original idea to try control the LSB developped over the two airfoil sides but, from the found results, this passive technique requires further work to will find its potential and demands more endeavors to know the best way how to apply it.

References

[1] A. Choudry, M. Arjouandi, R. Kelso, A study of long separation bubble on thick airfoil and its consequent effects, International Journal of Heat and Fluid Flow, 52 (2015) 84-96

[2] G.M.H. Shahariar, M.R. Hasan, M. Mashud, Laminar boundary layer separation control at leading edge of an airfoil, International Conference on Mechanical, Industrial and Energy Engineering, Khulna, Bengladesh, Dec. 26-27, 2014

[3] R. Mdouki, G. Bois, Numerical study of passive control with slotted blading in highly loaded compressor cascade at low Mach number, International Journal of Fluid Machinery and Systems, 4 (2011) 97-103

[4] R. Belamadi, A. Djemili, A. Ilinca, R. Mdouki, Aerodynamic performance analysis of slotted airfoils for application to wind blades, J. Wind Eng. Ind. Aerodyn. , 151 (2016) 79-99

[5] S.M.A. Aftab, A.S.M. Rafie, N.A. Razak, K.A. Ahmad, Turbulence model selection for low Reynolds number flows, Plos One Journal, 11 (2016) 1-15

[6] F. R. Menter, R. Langtry, S. Volker, Transition modelling for general purpose CFD codes, Flow turbulence combust, 77 (2006) 277-303

[7] R. R. Ramsay, M. J. Hoffmann, G.M. Gregorek, Effects of Grit Roughness and Pitch Oscillations on the S809 , The Ohio State University, December 1995, NREL/TP-442-7817

[8] P.W. Walter, S.O. Stuart, CFD calculations of S809 aerodynamic characteristics, AIAA, 35th Aerospace Sciences Meeting and Exhibit, Reno, NV, Jan. 6-9, 1997

[9] K. L. Hansen, R. M. Kelso, A. Choudry, M. Arjouandi, Laminar separation bubble effect on the lift curve slope of an airfoil, 19th Australian Fluid Mechanics Conference, Melbourne, Australia, Dec. 8-11, 2014

[10] M.S. Genç, U. Kaynac, Control of laminar separation bubble over a NACA2415 aerofoil at low Reynolds transitional flow using blowing/suction, 13th Aerospace Sciences & Aviation Technology, Cairo, Egypt, May. 26-28, 2009

[11] A.C.N. Tan, D. J. Auld, Study of laminar separation bubbles at low Reynolds number under various conditions, 11th Australian Fluid Mechanics Conference, Hobart, Australia, Dec. 14-18, 1992
[12] R. Azim, M.H. Hasan, M. Ali, Numerical investigation on the delay of boundary layer separation by suction for NACA 4412, Procedia Engineering, 105 (2015) 329-334
[13] M. Gul, O. Uzol, I.S. Akmandor, An experimental study on active flow control using synthetic jet actuators over S809 airfoil, Journal of physics: Conference series, 524 (2014)
[14] M. Jamahiri, Laminar separation bubble: its structure, dynamics and control, Research report 2011:06, Chalmers University of Technology, Goteborg, Sweden
[15] D. K. Walters, D. Cokljat, A Three-Equation Eddy-Viscosity Model for Reynolds-Averaged Navier–Stokes Simulations of Transitional Flow, Journal of Fluids Engineering, 130 (2006) 1-14
[16] P.B.S. Lissaman, Low Reynolds number airfoil, Ann. Rev. Fluid Mech. 15 (1983) 223-239